Sección Especial en Óptica Cuántica / Special Section on Quantum Optics

Quantum metrology with atoms and photons

Metrología cuántica con átomos y fotones

Federica A. Beduini[(1)], Naeimeh Behbood[(1)], Yannick de Icaza[(1)], Brice Dubost[(1)], Marco Koschorreck[(2)], Mario Napolitano[(1)], Ana Predojević[(3)], Robert Sewell[(1)] Florian Wolfgramm[(1)], Morgan W. Mitchell[(1,*)]

1. ICFO-Institut de Ciencies Fotoniques, Mediterranean Technology Park, 08860 Castelldefels (Barcelona), Spain.
2. University of Cambridge, Physics Department Cavendish Laboratory Cambridge CB3 0HE, United Kingdom.
3. Institut für Experimentalphysik, University of Innsbruck, Technikerstr. 25, A-6020 Innsbruck, Austria.

[(*)] Email: morgan.mitchell@icfo.es

Recibido / Received: 30/10/2010. Aceptado / Accepted: 15/12/2010

ABSTRACT:

We describe our recent work in quantum metrology using atomic and photonic systems for measurements with sensitivity beyond the standard quantum limit, e.g., beyond the shot-noise and projection-noise limits. We demonstrate two optical magnetometry systems using rubidium atoms as field sensors, with optical read-out by paramagnetic Faraday rotation. Our hot-atom magnetometer operates beyond the shot-noise limit of sensitivity using a polarization-squeezed optical probe. Our next-generation cold-atom magnetometer operates on similar principles but with much greater atomic control. We demonstrate quantum-non-demolition measurement of the collective spin of the atom cloud at both the shot-noise and projection-noise limits of sensitivity.

Keywords: Quantum Optics, Quantum Metrology, Optical Magnetometry, Squeezed Light, Polarization Squeezing, Cold Atoms, Spin Squeezing, Quantum Non-Demolition Measurement.

RESUMEN:

Se describe nuestro más reciente trabajo en metrología cuántica usando sistemas atómicos y fotónicos para medir con una sensibilidad por encima del límite cuántico estándar, es decir, por encima de el límite impuesto por el ruido de disparo y el ruido de proyección. Demostramos dos sistemas de magnetometría óptica que emplean átomos de rubidio como sensores del campo, leyendo ópticamente los átomos por la rotación de Faraday. El primero, formado por átomos calientes, opera más allá del límite de la sensibilidad por el ruido de disparo, usando como haz de prueba luz polarizada comprimida. El segundo, un magnetómetro de átomos fríos de siguiente generación, opera con principios similares pero con un alto control en los átomos. Demostramos medidas cuánticas no destructivas del espín colectivo de la nube de átomos y que están en el límite de la sensibilidad tanto del ruido de disparo como del ruido de proyección.

Palabras clave: Óptica Cuántica, Metrología Cuántica, Magnetómetros Ópticos, Luz comprimida, Luz Polarizada Comprimida, Átomos Fríos, Compresión de Espín, Medidas Cuánticas No Destructivas.

REFERENCES AND LINKS

[1]. G. Santarelli, Ph. Laurent, P. Lemonde, A. Clairon, A. G. Mann, S. Chang, A. N. Luiten, C. Salomon, "Quantum projection noise in an atomic fountain: A high stability cesium frequency standard", *Phys. Rev. Lett.* **82**, 4619 (1999).

[2]. V. Shah, G. Vasilakis, M. V. Romalis, "High bandwidth atomic magnetometery with continuous quantum nondemolition measurements", *Phys. Rev. Lett.* **104**, 013601, (2010).

[3]. S. Fairhurst, G. Guidi, P. Hello, J. Whelan, G. Woan, "Current status of gravitational wave observations", *Gen. Relat. Gravit.* **43**, 387-407 (2010).

[4]. H. Vahlbruch, S. Chelkowski, B. Hage, A. Franzen, K. Danzmann, R. Schnabel, "Demonstration of a squeezed-light-enhanced power- and signal-recycled Michelson interferometer", *Phys. Rev. Lett.* **21**, 211102 (2005).

[5]. K. Goda, O. Miyakawa, E. E. Mikhailov, S. Saraf, R. Adhikari, K. McKenzie, R. Ward, S. Vass, A. J. Weinstein, N. Mavalvala, "A quantum-enhanced prototype gravitational-wave detector", *Nat. Phys.* **4**, 472-476 (2008).

[6]. M. F. Riedel, P. Boehi, Y. Li, T. W. Haensch, A. Sinatra, P. Treutlein, "Atom-chip-based generation of entanglement for quantum metrology", *Nature* **464**, 1170-1173 (2010).

[7]. C. Gross, T. Zibold, E. Nicklas, J. Esteve, M. K. Oberthaler, "Nonlinear atom interferometer surpasses classical precision limit", *Nature* **464**, 1165-1169 (2010).

[8]. M. W. Mitchell, J. S. Lundeen, A. M. Steinberg, "Super-resolving phase measurements with a multiphoton entangled state", *Nature* **429**, 161-164 (2004).

[9]. I. Afek, O. Ambar, Y. Silberberg, "High-NOON states by mixing quantum and classical light", *Science* **328**, 879-881 (2010).

[10]. J. A. Jones, S. D. Karlen, J. Fitzsimons, A. Ardavan, S. C. Benjamin, G. Andrew D. Briggs, J. J. L. Morton, "Magnetic field sensing beyond the standard quantum limit using 10-spin NOON states", *Science* **324**, 1166-1668 (2009).

[11]. K. Banaszek, R. Demkowicz-Dobrzanski, I. A. Walmsley, "Quantum states made to measure", *Nat. Photonics* **3**, 673-676 (2009).

[12]. V. Giovannetti, S. Lloyd, L. Maccone, "Quantum metrology", *Phys. Rev. Lett.* **96**, 010401 (2006).

[13]. S. Boixo, S. T. Flammia, C. M. Caves, J. M. Geremia, "Generalized limits for single-parameter quantum estimation", *Phys. Rev. Lett.* **98**, 090401 (2007).

[14]. S. Boixo, A. Datta, M. J. Davis, S. T. Flammia, A. Shaji, C. M. Caves, "Quantum metrology: dynamics versus entanglement", *Phys. Rev. Lett.* **101**, 040403 (2008).

[15]. F. Wolfgramm, A. Cerè, F. A. Beduini, A. Predojević, M. Koschorreck, M. W. Mitchell, "Squeezed-light optical magnetometry", *Phys. Rev. Lett.* **105**, 053601 (2010).

[16]. J. Beltrán, A. Luis, "Breaking the Heisenberg limit with inefficient detectors", *Phys. Rev. A* **72**, 045801, (2005).

[17]. A. Negretti, C. Henkel, K. Mølmer, "Quantum-limited position measurements of a dark matter-wave soliton", *Phys. Rev. A* **77**, 043606, (2008).

[18]. M. J. Woolley, G. J. Milburn, C. M. Caves, "Nonlinear quantum metrology using coupled nanomechanical resonators", *New J. Phys.* **10**, 125018 (2008).

[19]. B. A. Chase, B. Q. Baragiola, H. L. Partner, B. D. Black, J. M. Geremia, "Magnetometry via a double-pass continuous quantum measurement of atomic spin", *Phys. Rev. A* **79**, 062107, (2009).

[20]. M. Napolitano, M. W. Mitchell, "Nonlinear metrology with a quantum interface", *New J. Phys.* **12**, 093016 (2010).

[21]. A. Predojevic, Z. Zhai, J. M. Caballero, M. W. Mitchell, "Rubidium resonant squeezed light from a diode-pumped optical-parametric oscillator", *Phys. Rev. A* **78**, 063820 (2008).

[22]. M. Kubasik, M. Koschorreck, M. Napolitano, S. R. de Echaniz, H. Crepaz, J. Eschner, E. S. Polzik, M. W. Mitchell, "Polarization-based light-atom quantum interface with an all-optical trap", *Phys. Rev. A* **79**, 043815 (2009).

[23]. M. Kubasik, M. Koschorreck, M. Napolitano, S. R. de Echaniz, H. Crepaz, J. Eschner, E. S. Polzik, M. W Mitchell, "Polarization-based light-atom quantum interface with an all-optical trap", *Phys. Rev. A* **79**, 043815 (2009).

[24]. P. J. Windpassinger, M. Kubasik, M. Koschorreck, A. Boisen, N. Kjaergaard, E. S. Polzik, J. H. Müller, "Ultra low-noise differential ac-coupled photodetector for sensitive pulse detection applications", *Meas. Sci. Technol.* **20**, 055301 (2009).

[25]. M. Koschorreck, M. Napolitano, B. Dubost, M. W. Mitchell, "Sub-projection-noise sensitivity in broadband atomic magnetometry", *Phys. Rev. Lett.* **104**, 093602 (2010).

[26]. L. Viola, S, Lloyd, “Dynamical suppression of decoherence in two-state quantum systems”, *Phys. Rev. A* **58**, 2733-2744 (1998).
[27]. L. Viola, E. Knill, S. Lloyd, “Dynamical decoupling of open quantum systems”, *Phys. Rev. Lett.* **82**, 2417-2421 (1999).
[28]. P. Facchi, S. Tasaki, S. Pascazio, H. Nakazato, A. Tokuse, D. A. Lidar, “Control of decoherence: Analysis and comparison of three different strategies”, *Phys. Rev. A* **71**, 22302 (2005).
[29]. M. Koschorreck, M. Napolitano, B. Dubost, M. W. Mitchell, “Quantum nondemolition measurement of large-spin ensembles by dynamical decoupling”, *Phys. Rev. Lett.* **105**, 093602 (2010).
[30]. M. Koschorreck, M. Napolitano, B. Dubost, M. W. Mitchell, “Sub-projection-noise sensitivity in broadband atomic magnetometry”, *Phys. Rev. Lett.* **104**, 093602 (2010).

1. Introducción

The most precise measurement instruments are interferometric in nature. Optical interferometers developed for detection of gravitational waves can measure the deformation of space-time with a phenomenal precision, better than 1 part in 1022. Atom interferometers follow the same interferometric principles, applied to interference of atomic states or atomic wave-functions. These achieve phenomenal precision in many other measurements: because atomic states evolve in response to a variety of influences, including gravitational, magnetic, electric, radio-frequency, and optical fields, they offer a versatile platform for ultra-sensitive measurement of the quantities of greatest physical interest.

Already, atomic clocks, atomic gravimeters and atomic magnetometers outperform any non-atomic technology in their respective areas, for example measuring time and frequency to 16 or more digits of precision, and measuring magnetic fields below the femto-tesla level. These already open new and surprising applications. Atomic clocks can detect the warping of space-time by the mass of the earth, and two clocks run at measurably different speeds when one is placed only 30 cm farther from the earth’s centre. State-of-the art magnetometers used in magneto-encephalography can observe brain activity in real-time, by detecting the ultra-weak magnetic fields produced by neural currents, with profound implications for medical diagnosis and fundamental science.

Soon, these instruments will reach the limits of classical technique, and their performance will be determined by quantum effects. Already, atomic clocks and atomic magnetometers approach the “standard quantum limit” (SQL)[1,2], as will the next generation of gravitational-wave detectors [3]. The science of manipulating quantum systems to achieve sensitivity beyond the SQL is the field of quantum metrology. The field has experienced an explosion in recent years, impelled by the demand from gravitational wave instruments for quantum-enhanced sensitivity [4,5], by new atomic techniques [6,7], by new methods for engineering metrologically-advantageous entangled states [8-11], by a general theoretical framework [12], and by proposals to go beyond the general framework [13,14].

In this article, we describe several experiments in the area of quantum metrology applied to atomic magnetometry; the measurement of magnetic fields using atoms. The article is organised as follows: in section 2 we discuss the quantum limits of metrology in general, and magnetometry in particular; in section 3 we present experimental results of atomic magnetometry with entangled photon sources; and in section 4 we demonstrate a shot-noise and projection-noise limited measurement of atomic spin using ultracold atoms.

2. Quantum physics of sensitivity

The fundamental limits of sensitivity are intimately tied to the nature of quantum physics. In general, quantum metrology problems are estimation problems, in which an unknown quantity χ cannot be directly measured, but it can be inferred from measurements on a quantum system influenced by that quantity. For example, χ might be a magnetic field, which influences a system of N photons through

Faraday rotation by an angle ϕ. By measuring the photons, we learn something about χ, limited by noise in the measurement.

In a single measurement we gain information about the signal $\langle\phi\rangle$. The noise $\Delta\phi$ is the RMS variation in the measured ϕ, also called the sensitivity of the measurement, because it is the smallest signal detectable with unit signal-to-noise ratio. We study both the *absolute sensitivity* that can be achieved in a measurement given a finite number of particles N, and also how this sensitivity *scales* as a function of N.

2.1 Technical noise

In quantum metrology, "technical noise" refers to noise sources which scale with N in the same way as the signal. For example, if the gain of a detector is fluctuating by 1%, it introduces a noise equal to 1% of the signal, whatever that signal might be. In this situation, increasing N doesn't change the signal-to-noise ratio. We have a scaling $\Delta\phi\propto N^0$.

Reducing technical noise improves sensitivity, but only until the technical noise drops below other, more fundamental, noise sources.

2.2 Standard quantum limit

Interferometers employ light and matter as waves, but at the moment of detection the particle-like nature of atoms and photons introduces randomness into the detected signal. The SQL, also known as shot noise in optics and projection noise in atomic ensembles, implies a sensitivity $\delta\phi\propto N^{-1/2}$ for a probe consisting of N *independent* particles. The SQL describes how the sensitivity of the best possible "standard" measurement, i.e., one which does not take advantage of quantum effects such as entanglement, scales with N.

Quantum mechanics offers new resources in metrology that allow us to make measurements that improve on the SQL by introducing correlations amongst the particles in the probe so that they are no longer independent particles but either interacting or entangled. This is the subject of the field of quantum metrology.

2.3 Entanglement-based metrology

The standard resource introduced into quantum metrology to beat the SQL is entanglement. If the probe system of N particles is prepared in an entangled state (e.g. a squeezed state) prior to making the measurement, then correlations amongst the N particles can reduce the noise introduced in the measurement. Allowing for entanglement, non-interacting particles are constrained by the much weaker "Heisenberg limit" (HL), sensitivity $\delta\phi\propto N^{-1}$. The HL is also a consequence of fundamental physics, in this case the uncertainty principle. For a given Hamiltonian, the HL describes how the sensitivity of the best possible quantum measurement scales with N.

In a typical measurement N can be very large (many photons or atoms), so the potential benefits of improving on the SQL are large. Prototype gravitational wave detectors incorporating squeezing, a macroscopic manifestation of entanglement, have already demonstrated sensitivity enhancements beyond the SQL [4,5], and the next generation of gravitational wave detectors will incorporate squeezed light components [3]. In our laboratory we have demonstrated a prototype squeezing-enhanced magnetometer [15] (see section 3 below).

2.4 Quantum metrology beyond entanglement

Theoretical quantum metrology has produced both a standard model of quantum metrology [12] and proposals to go *beyond* the standard model. Notable among these is the observation that the HL can be overcome if an additional resource, *interaction* among particles, is present [13,14]. Interactions lead to nonlinear terms in the Hamiltonian describing the coupling between the probe system and the parameter of interest. A carefully engineered nonlinear Hamiltonian can be used to amplify the measurement signal without introducing significant excess noise. For a k-particle interaction, the limiting sensitivity is $\delta\phi\propto N^{-k+1/2}$ without entanglement, and $\delta\phi\propto N^{-k}$ with entanglement. Proposals for metrologically-relevant nonlinearities include Kerr nonlinearities [16], cold collisions [14] and topological excitations [17] in Bose condensates, Duffing nonlinearity in nano-mechanical resonators [18], and a two-pass effective nonlinearity with an atomic ensemble [19]. We have recently proposed a method to test nonlinear metrology in an atomic ensemble [20]. The enhanced scaling of nonlinear quantum metrology offers the promise of spectacular improvements in measurement sensitivity if the scaling persists to sufficiently large *N*.

2.5 Quantum metrology in magnetometry

In our laboratory we study a prototypical measurement: atomic magnetometry. A schematic atomic magnetometer is illustrated in Fig. 1. In such an experiment, an ensemble of atoms is used to measure a weak external magnetic field. The atoms may be held in a vapour cell at room temperature, or laser cooled to micro-Kelvin temperatures and trapped in an optical dipole potential. The coupling between the atoms and the magnetic field is described by the Zeeman interaction: $\hat{H}_{mag} = \mu \vec{B} \cdot \vec{F}$, where μ is the magnetic moment of the atom and $\vec{F}$ is the collective atomic spin. In a typical experiment, the atomic ensemble is first spin polarised along the x direction via optical pumping. The collective spin will then precess toward z in response to the field component B_y, and the F_z component is detected optically using the paramagnetic Faraday effect and a polarimeter. The magnetometer can be understood as an interferometer: the initial state of the atoms, aligned along x, is a superposition of non-degenerate eigenstates of the Hamiltonian, which acquire differing phases during the evolution. These phases are transferred to the $\sigma_{+,-}$ components of a linearly polarised optical probe, and detected as a polarization rotation.

There are two sources of quantum noise which are important in such an experiment: the shot noise associated with the probe light, and the projection noise of the atomic ensemble. A fully optimised "standard" measurement operating at the SQL will be both shot noise and projection noise limited. Improving the magnetometer beyond the SQL requires reducing one or both of these noise sources by engineering entanglement of the photonic and/or atomic states. Here we report on experimental studies of squeezed states of both systems. A squeezed state is a macroscopic entangled state in which quantum fluctuations of the N particle system are correlated in such a way as to reduce quantum noise in the measurement.

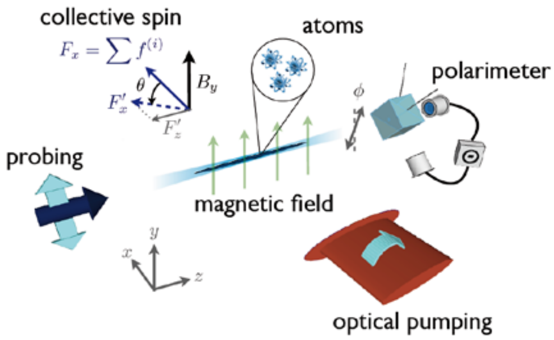

Fig. 1: Optical magnetometer: The collective spin $\vec{F}$ of an ensemble of atoms is prepared along the x direction, and allowed to precess toward z in response to the field component By. The F_z component is detected optically, using the paramagnetic Faraday effect and a polarimeter. The magnetometer can be understood as an interferometer: the initial state of the atoms, aligned along x, is a superposition of non-degenerate eigenstates of the Hamiltonian $\propto \vec{B} \cdot \vec{F}$ which acquire differing phases during the evolution.

3. Photonic entanglement in magnetometry: polarization squeezing

The signal that is ultimately detected in an atomic magnetometer is the polarization of the optical probe. The precision with which we can measure the polarization state can be improved by preparing the optical probe in type of entangled state called a polarization squeezed state. In such a state, the noise associated with component of the Stokes vector $\vec{S}$ describing the polarization of the optical probe (the one detected in the experiment) is reduced at the expense of increasing the noise in an orthogonal component.

Using single-frequency lasers, frequency conversion, and low-loss optics, we have demonstrated generation of polarization-squeezed light resonant with the D_1 line of ^{87}Rb [21]. First, we generate vertically-polarized quadrature squeezed light using a sub-threshold degenerate optical parametric oscillator (OPO).

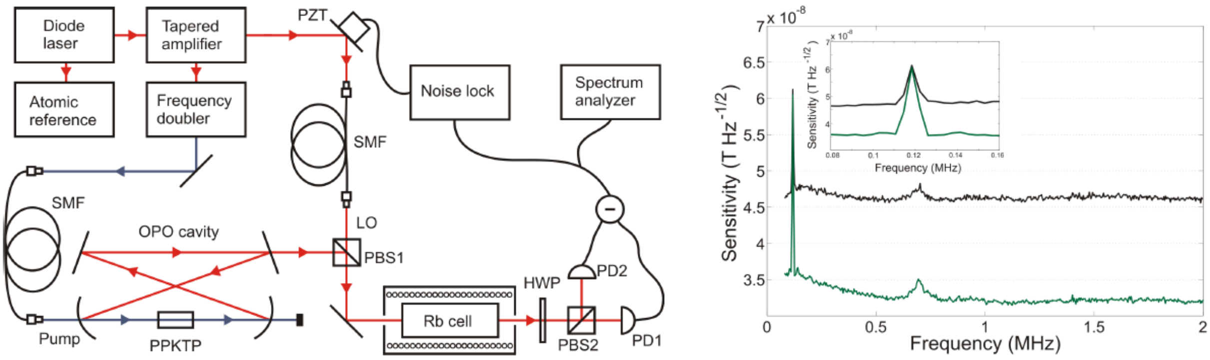

Fig. 2: Left: Schematic of polarization squeezing and hot-atom magnetometer. Rb cell, rubidium vapor cell with magnetic coil and magnetic shielding; OPO, optical parametric oscillator; PPKTP, phase-matched nonlinear crystal; LO, local oscillator beam; PBS, polarizing beam splitter; HWP, half-wave plate; SMF, single-mode fiber; PD, photodiode. Right: Magnetometer noise level for shot-noise-limited (upper curve) and squeezing-enhanced (lower curve) operation. The signal at 120 kHz, produced by a magnetic field coil, is used for calibration. From [15].

Vacuum fluctuations enter the OPO, and by a process of phase-sensitive amplification, the noise of one quadrature is reduced at the expense of the other quadrature. This produces vertically polarized "squeezed vacuum," which is combined with horizontally-polarized laser light. The interference of the two polarizations produces polarization squeezing: the laser field plus one quadrature gives the +45°/–45° power balance $\hat{S}_y$, laser plus the other quadrature gives the left circular/right circular balance $\hat{S}_z$. Squeezing of a quadrature thus produces squeezing of one polarization component.

The suitability of the source for quantum metrology was recently demonstrated by improving the sensitivity in a shot-noise-limited atomic magnetometer with room temperature atoms in a vapour cell [15]. The experimental setup is shown schematically in Fig. 2. The principal light source is an external cavity diode laser at 794.7 nm, tunable over the D_1 transition of atomic rubidium. The frequency is stabilized to individual transitions of the D_1 line of Rb by FM saturated absorption spectroscopy. The laser output passes through a tapered amplifier and is split in two parts: The weaker part is spatially filtered with a single-mode fiber and serves as local oscillator (LO) beam. The stronger part is frequency doubled to 397.4 nm and then sent through a single-mode fiber for mode-cleaning. This is used to pump a subthreshold optical parametric oscillator (OPO) producing squeezed vacuum. The nonlinear medium in the OPO is a type-I phase-matched PPKTP crystal. The cavity is actively stabilized by using a frequency-shifted beam with a polarization orthogonal to the polarization of the squeezed vacuum.

The vertically-polarized cavity output is combined with the horizontally-polarized LO at a polarizing beam splitter (PBS1) with a 99% degree of overlap. The resulting light is horizontally polarized, with squeezed fluctuations in the diagonal or circular polarization basis.

The polarization-squeezed light is then sent through a 15 cm-long atomic vapour cell at room temperature. The isotopically purified atomic vapor contains >99% ^{87}Rb with a small concentration of ^{85}Rb. We lock the laser to the $5^2S_{1/2}(F=3)\rightarrow 5^2P_{1/2}(F'=2)$ transition of the D_1 line of ^{85}Rb. This corresponds to a detuning of about 700 MHz from the closest 87Rb resonance. The cell is contained within a single-layer μ-metal cylinder to shield external magnetic fields while a coil within the cylinder generates the desired field B_z.

The optical rotation is detected by a shot-noise limited polarimeter: after a half-wave plate at 22,5°, a polarizing beam splitter (PBS2) splits the horizontally and vertically polarized components of the beam and directs them to the two photodiodes of a balanced amplified photo-detector with a quantum efficiency of 95%. Quantum noise locking is used to stabilize the phase of the local oscillator at maximum squeezing or anti-squeezing.

As shown also in Fig. 2, before the squeezing is applied, i.e., with the pump laser off, the noise floor of the magnetometer is at the SQL, i.e., limited by quantum polarization noise. When the squeezing is applied, the noise floor drops, and the signal-to-noise ratio improves, indicating the value of squeezing in an atomic magnetometer.

4. Atomic entanglement in magnetometry: spin squeezing

Because an atomic magnetometer involves two quantum systems, the atoms and the light which is used to detect the atoms, it is advantageous also to squeeze (and thus generate entanglement in) the ensemble of atomic spins. Precise measurement of atomic spin is a challenging task; to accomplish this we use extremely well-controlled atoms, laser cooled to μK temperatures and held in an all-optical (and hence non-magnetic) trap.

4.1 A cold-atom magnetometry system

A schematic of our experimental system to generate ultra-cold, magnetically-sensitive atomic ensembles is shown in Fig. 3(a). The system is designed to hold a sample of about one million ^{87}Rb atoms in an optical dipole trap for very efficient interaction with near-resonant light. After laser cooling to about 25 μK, the atoms are loaded into the weakly-focused beam of a Yb:YAG laser at 1030 nm. Tight (weak) confinement in the transverse (longitudinal) direction produces a sample with high aspect ratio of $\simeq 240:1$. This geometry ensures that light propagating along the trap axis interacts very strongly with the atomic system. The figure of merit for this interaction is the effective on-resonance optical depth, which is above 50 in our setup [22].

This is a versatile experimental system: it allows us to efficiently optically pump the atomic ensemble either from the side or along the trap axis, to image the ensemble from the side to count the number of atoms and gain information about the temperature and density distribution of the ensemble, and to detect the spin state of the ensemble with appropriately linearly polarised light propagating along the trap axis. For this experiment we sue light resonant with various transitions on the $5^2S_{1/2}\rightarrow 5^2P_{3/2}D_2$ line of ^{87}Rb, as shown in Fig. 3(b).

In a typical experimental sequence, the atoms are loaded into the trap, prepared in the $5^2S_{1/2}$ (F=1) ground state and optically pumped into a specific spin state in the F=1 spin manifold. Depending on the experiment, this may be a polarized state with the total spin $\vec{F}$ along a given direction, or an aligned state with the pseudo-spin $\hat{\mathbf{J}}$ along a given direction. $\hat{\mathbf{J}}\equiv(\hat{S}_x,\hat{S}_y,\hat{S}_z)/2$, where the Pauli matrices σ_i act on the $\left|F=1,m_F=\pm1\right\rangle$ subspace. Optical probing by paramagnetic Faraday rotation measures the component $\hat{F}_z=2\hat{J}_z$ of the collective spin.

4.2 Optical QND measurement

The paramagnetic Faraday interaction can be described by a simple Hamiltonian

$$\tau\hat{H}_{eff}=G_1\hat{S}_z\hat{J}_z+G_2\left(\hat{S}_x\hat{J}_x+\hat{S}_y\hat{J}_y\right), \qquad (1)$$

where τ is the duration of the pulse and $G_{1,2}$ are coupling constants that depend on the atomic absorption cross section, the beam geometry, the detuning from resonance Δ, and the hyperfine structure of the atom [23]. The atomic variables $\hat{\mathbf{J}}$ are collective spin and alignment operators related to the total atomic spin $\hat{\mathbf{F}}$. The light is described by the Stokes operators $\hat{\mathbf{S}}$ defined as $\hat{S}_i=\frac{1}{2}(\hat{a}_+^\dagger,\hat{a}_-^\dagger)\sigma_i(\hat{a}_+,\hat{a}_-)^T$, where the σ_i are the Pauli matrices and $\hat{a}_\pm$ are annihilation operators for the temporal mode of the pulse and circular plus/minus polarization.

The G_1 term in the Eq. (1) describes a *quantum non-demolition* (QND) measurement. We can think of it as a making a weak projective measurement of the atomic variable $\hat{F}_z=(\hat{J}_z)$ without perturbing the atomic system. We can make many thousand quantum non-demolition (QND) measurements without significantly damaging the atomic spin state. The G_2 term describes a more complicated coupling which is discussed further below.

In the following section we show results that demonstrate that the experiment is both shot noise and projection noise limited - i.e. operating at the quantum limit for both systems.

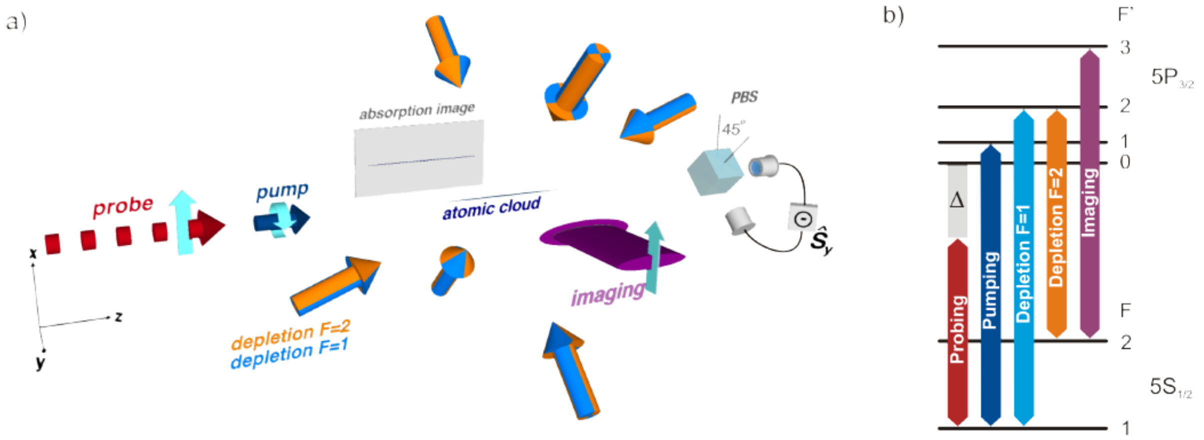

Fig. 3: a) Atomic ensemble with probing, pumping, and imaging light fields. The polarimeter measures in the 45º-basis, i.e., the Stokes component S_y; b) Atomic transitions for probing, preparation, and imaging light fields.

Furthermore, the QND interaction generates entanglement in the atomic system, producing a spin squeezed atomic state with reduced quantum noise in the $\hat{F}_z = (\hat{J}_z)$ variable, allowing us to improve the measurement sensitivity beyond the SQL.

4.3 Thermal spin state calibration

In order to establish that we can make a projection noise limited measurement of the atomic spin state, we first calibrate the measurement using a well defined input state, the thermal spin state (TSS) as a noise source. This state has an average spin $\langle \vec{F} \rangle = 0$, making it insensitive to technical noise sources such as ambient magnetic field fluctuations, and a well defined quantum noise var($\hat{F}_z$)= $N_A F(F+1)/3$, where N_A is the number of atoms in the ensemble. Calibration results are shown in Fig. 4.

The measurement of F_z is made by sending a train of 1 μs long pulses with 10 μs period to the atoms. Each pulse contains about 25×10^6 photons, vertically polarized and tuned 800 MHz to the red of the F=1→F'=0 transition. The output pulses are analyzed in the -45º basis with an ultra-low-noise balanced photo-detector [24], giving a direct measure of S_y. This signal is recorded on a digital storage oscilloscope for later evaluation. The optical probing system is shot-noise limited. Due to the high optical density, the measurement achieves a sensitivity of ≈ 500 spins, better than the projection noise level for the system.

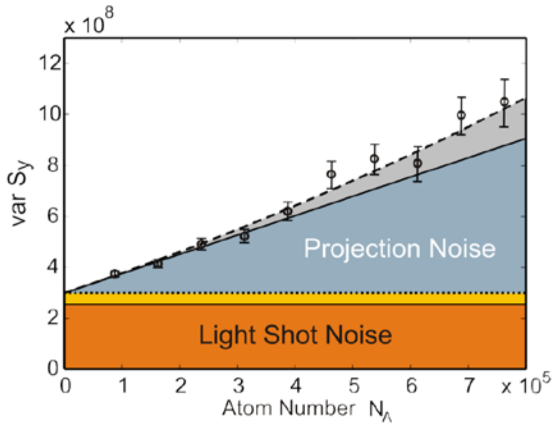

Fig. 4: Measured variance of $\hat{S}_y$ with statistical errors for N_L=10^9 as a function of atom-number. Dashed curve: Theoretical curve including technical noise sources. Solid Line: Pure spin quantum noise. Dotted Line: Shot noise and technical light noise, Thin solid line: Light shot noise. The electronic noise is not plotted because it is negligible for this number of photons. From [25].

4.4 Dynamical decoupling

Achieving QND performance with a magnetically sensitive spin state, such as an $\hat{F}_x = (\hat{J}_x)$ polarised coherent spin state (CSS), requires that we take into account the G_2 term described in Eq. (1). This term describes a more complicated atom-light coupling that spoils the QND measurement, allowing spin changing interactions and coupling technical noise into the atomic spin state. In order to null the effect of this term in the Hamiltonian, we have designed a two-pulse probing scheme based on dynamical decoupling techniques[26-28]. This technique minimises decoherence in the atom-light interaction by effectively eliminating the G_2 terms, while keeping the G_1 term[29].

We demonstrate the effectiveness of this technique by measuring a $\hat{J}_x$-polarized CSS [30]. In each measurement cycle the atom number N_A is first measured by a dispersive atom-number measurement (DANM). We then prepare the CSS and probe with pulses of alternating polarization to find the QND signal $\hat{S}_y \equiv \sum_i \hat{S}_{y,i}^{(out)}(-1)^{i+1}$. Immediately after, $\langle \hat{J}_x \rangle$ is measured to quantify depolarization of the sample and any atoms having made transitions to the F=2 manifold are removed from the trap, reducing N_A for the next cycle and allowing a range of N_A to be probed on a single loading. This sequence of state preparation and probing is repeated ten times for each loading of the trap. The trap is loaded 350 times to acquire statistics.

Results, indicating projection-noise-limited QND measurement, compared to naive without the dynamical decoupling technique (which does not achieve the SQL), are shown in Fig. 5.

4.5 Spin squeezing in magnetometry

A projection-noise limited QND measurement, as demonstrated above, leaves the atomic system in a reduced-uncertainty state and is capable of generating spin squeezing. To employ this for magnetometry, the atoms will first be polarized by optical pumping, with $\vec{F}$ along the x-axis. Then a first measurement of the projection F_Z will be made by QND measurement. This collapses the ensemble into a spin-squeezed state, with reduced uncertainty in F_Z, and thus greater sensitivity to Larmor precession. Successive QND measurements both indicate the rotation angle and thus the field, and again produce spin squeezing.

5. Conclusions

Quantum physics has the potential to improve the performance of the most sensitive atomic interferometers, including atomic clocks and atomic magnetometers. We have demonstrated quantum-enhanced sensitivity of an atomic magnetometer, one using hot atoms and polarization-squeezed light. This achieves sensitivity below the shot-noise limit, showing the utility of optical squeezing in magnetometry.

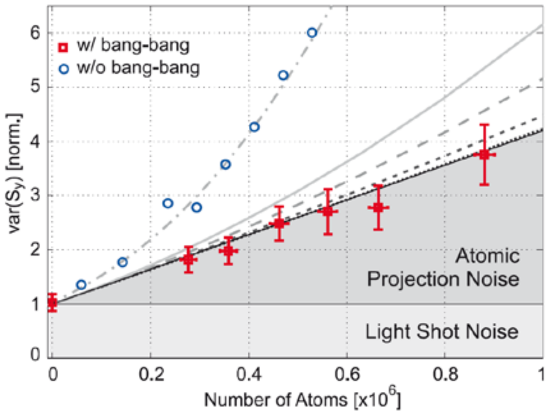

Fig. 5. Variance of polarimeter signal as a function of atom number, comparing probing with naive (single input polarization), or dynamically-decoupled probing with alternating polarization with p alterations per cycle. Grey curves indicate simulation results for: naive probing (solid), and decoupled probing with p=1 (widely dashed), p=2 (dashed), and p=5 (dotted). The black solid line shows the expected projection noise for $p\rightarrow\infty$, or the ideal QND interaction G_2=0. All curves are calculated using the independently measured interaction strength G_1=1.27(5)×10^{-7} and have no free parameters. Red squares are measured data using dynamical decoupling with p=5. Blue circles are measured data with naive probing. Technical noise from laboratory fields dominates the naive probing results, and pushes them above the theoretical curve, while technical noise is suppressed in the dynamically-decoupled probing. From [29].

A cold atomic ensemble, using laser-cooled rubidium and an all-optical trap, is the basis for a next-generation magnetometer. In this system we have demonstrated quantum non-demolition measurement of the atomic ensemble spin, with a precision at the dual quantum limits of optical shot noise and atomic projection noise. These are essential ingredients for the next step in sensitivity improvement, squeezing of the quantum fluctuations of the atoms themselves, “spin squeezing.”

Acknowledgements

This work was supported by the Ministry of Science and Innovation under the ILUMA project (Ref. FIS2008-01051) and the Consolider-Ingenio 2010 Project “QOIT” and Ingenio-Explora project OCHO (Ref. FIS2009-07676-E/FIS). RJS is acknowledges support of the Marie Curie RTN “EMALI.” FW and AP are supported by the Commission for Universities and Research of the Department of Innovation, Universities and Enterprises of the Catalan Government and the European Social Fund.

